Phys. Status Solidi C **7**, No. 10, 2544–2547 (2010) / **DOI** 10.1002/pssc.200983914

physica status solidi c
www.pss-c.com
current topics in solid state physics

High-performance nanoparticle-enhanced tunnel junctions for photonic devices

Adam M. Crook[*], **Hari P. Nair, and Seth R. Bank**

Microelectronics Research Center, University of Texas at Austin, 10100 Burnet Rd, Austin TX, 78759, USA

Received 6 October 2009, accepted 11 May 2010

Keywords III-V semiconductors, nanoparticles, photoluminescence, tunnel junction devices

We describe GaAs-based tunnel junctions that are compatible with photonic devices, including long-wavelength vertical-cavity surface-emitting lasers and multi-junction solar cells. Tunneling was enhanced with semimetallic ErAs nanoparticles, particularly when grown at reduced substrate temperatures. Additionally, we present the first direct measurement of the quality of III-V layers grown above ErAs nanoparticles. Photoluminescence measurements indicate that III-V material quality does not degrade when grown above ErAs nanoparticles, despite the mismatch in crystal structures. These findings validate these tunnel junctions as attractive candidates for GaAs-based photonic devices.

1 Introduction Low-loss tunnel junctions are essential for a number of optoelectronic devices, particularly for interconnecting the junctions of solar cells and minimizing electrical/optical losses in vertical-cavity surface-emitting lasers (VCSELs) [1]. They are especially attractive for longer wavelength lasers because performance fundamentally degrades due to increasing p-type free carrier absorption (FCA) with wavelength [2,3]. High-performance InP-based VCSELs have been demonstrated without p-type distributed Bragg reflector (DBR) mirrors and operate at the telecommunication wavelength range (1.3-1.6 µm) [3]. This was accomplished by utilizing intracavity contacts and type II AlInAs/InP tunnel junctions. However, InP-based VCSELs suffer from the poor thermal conductivity of the available DBR layer materials [4]. Monolithic GaAs-based VCSELs offer a promising alternative to InP-based lasers for low cost telecommunication laser sources [5]. GaAs substrates offer significant advantages over InP, due to the high thermal conductivity and large index contrast of AlAs/GaAs DBRs, as well as the availability of lateral oxide apertures for current and optical confinement. Electrical resistance of the p-type DBR is problematic, however, due to the large valence band offsets between AlAs and GaAs [6]. The high p-doping that is necessary for low resistance p-DBRs causes significant free-carrier absorption loss at 1.55 µm, degrading threshold current and wall-plug efficiency [7]. Unfortunately, tunnel junctions grown on GaAs substrates suffer from a number of materials-related limitations such as the difficulty in achieving high active n-type carrier concentrations [8], and a lack of a favorable band alignment, such as the type-II InP/InAlAs heterointerface for InP-based devices [9].

Tunnel junctions enhanced with semimetallic ErAs nanoparticles have shown promise as an alternative to conventional tunnel junction technologies on GaAs. They have enhanced the performance of AlGaAs/GaAs tandem solar cells [10]. The performance of the top (AlGaAs) cell indicates that high-quality III-V material may be grown over ErAs; however this has not been directly investigated. While transmission electron microscopy studies are encouraging [11], the quality of the overgrown III-V material remains an open question due to the mismatch in crystal structures between the rocksalt ErAs nanoparticles and the zincblende III-V. Additionally, at these growth temperatures of 580 °C, the tunnel junctions grown have pro-

---

[*] Corresponding author: e-mail acrook@mail.utexas.edu, Phone: +00 512 471 5383, Fax: +00 512 471 9674

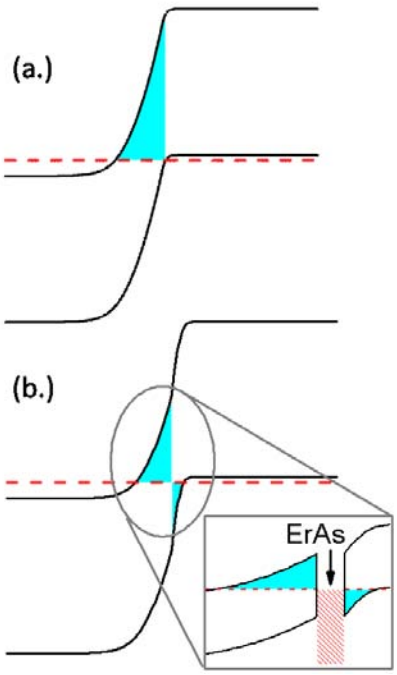

Figure 1 Equilibrium band diagrams for conventional (a.) and ErAs nanoparticle-enhanced (b.) GaAs tunnel junctions. The shaded regions represent the barrier(s) to current flow. Inset shows the band alignment of GaAs with the ErAs nanoparticles.

hibitively large resistivities [10,12] for use in VCSELs (~1kA/cm^2) [9] and concentrator solar cells [13].

We describe GaAs-based ErAs nanoparticle-enhanced tunnel junctions that meet the electrical requirements for both long-wavelength VCSELs and ultra high concentration (>500x) solar cells. We also present the first direct measurement of the optical quality of layers grown above ErAs nanoparticles. Photoluminescence studies indicate that InGaAs/GaAs quantum wells grown above ErAs nanoparticles are of comparable quality to those grown directly on a GaAs substrate.

These results indicate that ErAs nanoparticle-enhanced tunnel junctions offer great promise for enhancing photonic devices.

While this paper only examines ErAs nanoparticles embedded in GaAs, the plethora of semimetallic rare earth monopnictides span the lattice constants of III-V substrates [14]. In principle, this approach could be extended to tunnel junctions on any III-V substrate.

2 Nanoparticle-enhanced tunnel junction Traditional semiconductor tunnel junctions consist of highly-doped p+/n+ junctions where quantum mechanical band-to-band tunnelling enables classically forbidden current flow. Under forward bias operation, a traditional tunnel junction exhibits an Esaki peak (and negative differential resistance) which can degrade the conversion efficiency of multi-junction solar cells at high concentration levels [13]. The resistivity of the tunnel junction depends on the probability of a band-to-band tunnelling event: with a dependency on both the height and width of the potential barrier (illustrated in Fig. 1a). Reducing the resistivity of traditional tunnel junctions requires abrupt doping profiles, high doping concentrations, and a small bandgap. In multi-junction solar cells, the bandgap of the tunnel junction between series connected cells is limited by the absorption of the cells above the tunnel junction. Parasitic absorption in the solar cell reduces both the forward voltage and collected current from the multi-junction solar cell, by adding series resistance and reducing photon flux to be absorbed by underlying cells. A practical problem also occurs with obtaining high active n-type carrier concentrations on GaAs. For example, Si-doped GaAs is practically limited to a free electron concentration of ~5x10^{18} cm^{-3} [8]. Dopants such as tellurium can produce somewhat higher active concentrations, but are undesirable because of their high diffusivity and vapor pressure. These properties may corrupt doping profiles and increase background carrier concentrations, degrading device performance.

Most rare earth monopnictides (e.g. ErAs and ErSb) are rocksalt semimetals that may be embedded as epitaxial nanoparticles within a III-V matrix. As illustrated in Figure 1, embedding these nanoparticles at the tunnel junction interface pins the Fermi-level at the interface of the p-n junction, essentially creating back-to-back Schottky contacts. The back-to-back contacts allow tunnelling to occur via a two-step process, effectively halving the tunnelling distance for each step, dramatically increasing tunnel currents [12].

3 Electrical results Tunnel junctions were grown in a Varian GEN II solid-source molecular beam epitaxy (MBE) system on silicon-doped GaAs (100) substrates (electron concentration of 1-1.5x10^{18} cm^{-3}). Silicon and beryllium were used as n-type and p-type dopants, respectively. ErAs nucleates on GaAs in the Volmer-Weber (islanding) mode. The islands grow to a height and width of ~4 monolayers (ML) and then grow laterally outwards to form a complete film [11]. The amount of ErAs deposited was kept well below 4 ML so that a portion of the underlying GaAs matrix was exposed to seed the GaAs overgrowth of these rocksalt ErAs islands.

Samples were processed into mesa contact structures. Top Ohmic contacts in the form of a circular contact were evaporated using Pd/Ge/Ti/Pt/Au. The back Ohmic contact was formed using evaporated Pd/Ti/Pd/Au on the entire back of the sample. Devices were annealed in forming gas for 1 minute at 450 °C. The remainder of the p-GaAs contact layer was removed after metallization using citric acid:H_2O_2. Tunnel junction resistivity was extracted by the method in Denhoff [15]. With our device structure and measurement limitations, we calculated a lower bound for the measureable tunnel junction resistivity of ~5x10^{-5} Ω-cm^2.

As shown in Fig. 2, growing at reduced substrate temperature of 530 °C achieved high performance GaAs/ErAs/GaAs tunnel junctions with resistivity ~10^{-4} Ω-cm^2 (<0.25 V drop for current densities >10^3 A/cm^2). The current vs. voltage relations plotted in Figure 2 show an ~100x improvement over the results of Refs. [10] and [12]. The >10^3A/cm^2 current density is sufficient for incorporation into long-wavelength VCSELs to reduce the optical loss and series resistance associated with the p-type DBR. These ErAs nanoparticle-enhanced tunnel junctions add a trivial amount of voltage drop compared to optimized AlAs/GaAs DBR mirrors that use modulation doping to minimize series resistance, giving ~1 V at 1 kA/cm^2 [6].

The improvement in conductivity of the ErAs-enhanced tunnel junctions grown at reduced substrate temperature may be due to a combination of effects related to the nanoparticle size and morphology. In particular, lower growth temperature produces a higher density of smaller nanoparticles [16]. The morphology affects the energy band alignment between the ErAs and III-V, enhancing the conductivity. A detailed discussion will be presented in a separate publication [17].

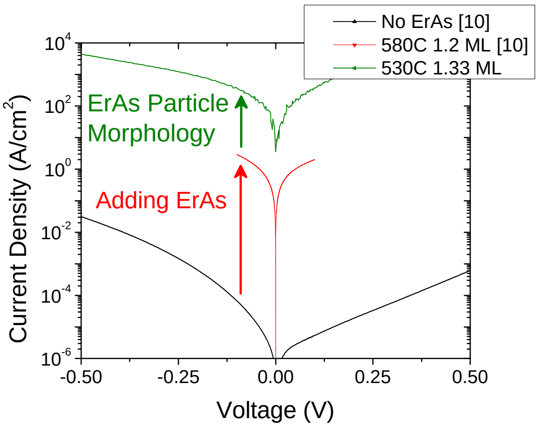

Figure 2 Current density and voltage for GaAs tunnel junctions showing the enhancement in tunnel current by adding ErAs (reproduced from Zide et. al., Ref. [10]) and further improvement with reduced growth temperature achieved in this work.

4 Optical quality of overgrowth With the dramatic improvement in tunnelling resistance achieved by growing at lower substrate temperatures, it is important to confirm that high-quality III-V overgrowth of the nanoparticles is possible under these growth conditions. This is an open question given the mismatched crystal structures of GaAs and ErAs. Additionally, overgrowth of complete films of ErAs results in anti-phase domain formation. While anti-phase domains can be avoided by limiting the ErAs layer to less than 2ML of deposition (less than 50% surface coverage) and seeding the overgrowth with the underlying GaAs [11], the optical quality of the overgrown III-V has not been directly studied.

In order to verify the optical quality of the layers grown on top of the ErAs nanoparticles, photoluminescence (PL) intensity was measured on optically excited InGaAs quantum well (QW) structures grown both with and without nanoparticle overgrowth as shown in Fig. 3. Because ErAs acts as an efficient nonradiative recombination center, a pn junction was used after the ErAs containing layer to block the diffusion of optically generated carriers to the ErAs nanoparticles. This enabled the quality of the InGaAs QWs to be directly compared. Samples were optically excited under 50 kW/cm^2 power density with 514 nm argon laser. PL intensity was measured with a germanium photodetector and a lock-in amplifier.

As seen in Fig. 4, the PL sample grown on top of ErAs nanoparticles exhibited PL intensity comparable to the sample grown without ErAs nanoparticles. The strength of the PL signal is indicative of high optical quality material with defect densities comparable to those of typical III-V layers.

The difference in the emission wavelength of the InGaAs QWs between the two samples is attributed to a change in the indium concentration. This is believed to originate from source drift during MBE growth, and not from the overgrowth of ErAs. The substrate peak is visible for each sample at ~870 nm. At lower excitation densities, the ratio of the InGaAs-to-GaAs peak height increases for the sample without ErAs, indicating that thermal escape of carriers from the QW could be responsible for the more pronounced substrate peak.

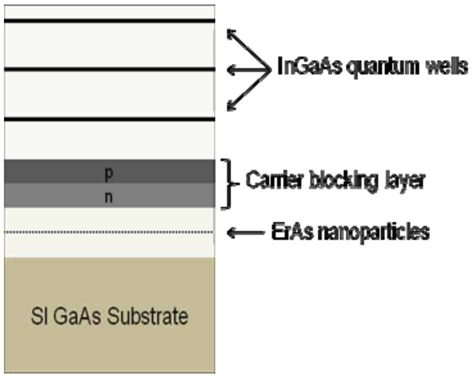

Figure 3 InGaAs/GaAs photoluminescence structures grown at 520°C, with and without an underlying layer of 1.33ML of ErAs nanoparticles.. The carrier blocking layer was utilized to prevent photogenerated carriers from diffusing to ErAs and recombining, enabling the quality of the InGaAs QWs to be directly investigated.

5 Conclusions Embedding ErAs semimetallic nanoparticles at the interface of GaAs tunnel junctions dramatically improved tunnelling current under both forward and reverse bias operation. By growing the ErAs nanoparticles at sufficiently low temperatures, we have

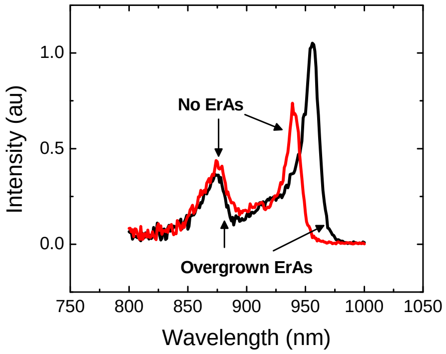

Figure 4 Normalized photoluminescence intensity spectrum for the PL structure shown in Fig. 3, with and without underlying ErAs nanoparticles. The comparable luminescence from the InGaAs QW peaks (~950 nm) indicates that ErAs nanoparticles do not degrade the optical quality of III-V grown above them.

demonstrated tunnel junctions with >1 kA/cm^2 current densities. We have also demonstrated that InGaAs/GaAs layers grown on ErAs nanoparticles have comparable optical quality to conventional InGaAs/GaAs material. With these promising results, future work will include the incorporation of ErAs nanoparticle enhanced tunnel junctions in long-wavelength VCSELs and GaAs based multi-junction solar cells, as well as the investigation of similar tunnelling structures on other III-V substrates, such as GaSb and InP.

Acknowledgements The authors acknowledge Professors Arthur Gossard and Joshua Zide for many useful discussions. This work was supported by the U. S. Army Research Office (ARO) through Grant No. W911NF-07-1-0528 and the Defense Advanced Research Projects Agency (DARPA) through the Young Faculty Award Program.

References

[1] M. Mehta, D. Feezell, D. Buell, A. W Jackson, L. A Coldren, and J. E Bowers, IEEE J. Quantum Electron. **42**, 675 (2006).

[2] C. H. Henry, R. A. Logan, F. R. Merritt, and J. P. Luongo, IEEE J. Quantum Electron. **19**, 947-952 (1983).

[3] S. Nakagawa, E. Hall, G. Almuneau, J. K. Kim, D. A. Buell, H. Kroemer, and L. A. Coldren, Appl. Phys. Lett. **78**, 1337 (2001).

[4] G. Almuneau, E. Hall, T. Mukaihara, S. Nakagawa, C. Luo, D. R. Clarke, and L. A. Coldren, IEEE Photon. Technol. Lett. **12**, 1322-1324 (2000).

[5] J. S. Harris Jr., IEEE J. Select. Top. Quantum Electron. **6**, 1145-1160 (2000).

[6] M. G. Peters, B. J. Thibeault, D. B. Young, A. C. Gossard, and L. A. Coldren, J. Vacuum Sci. Technol. B: Microelectron. Nanometer Struct. **12**, 3075-3083 (1994).

[7] A. Karim, S. Björlin, J. Piprek, and J. E Bowers, IEEE J. Select. Top. Quantum Electron. **6**, 1244-1253 (2000).

[8] S. Ahmed, M. R. Melloch, E. S. Harmon, D. T. McInturff, and J. M. Woodall, Appl. Phys. Lett. **71**, 3667-3669 (1997).

[9] J. S. Harris, S. R. Bank, M. A. Wistey, and H. B. Yuen, IEE Proc., Optoelectron. **151**, 407 (2004).

[10] J. M. O. Zide, A. Kleiman-Shwarsctein, N. C. Strandwitz, J. D. Zimmerman, T. Steenblock-Smith, A. C. Gossard, A. Forman, A. Ivanovskaya, and G. D. Stucky, Appl. Phys. Lett. **88**, 162103 (2006).

[11] C. Kadow, J. A. Johnson, K. Kolstad, J. P. Ibbetson, and A. C. Gossard, J. Vac. Sci. Technol. B **18**, 2197 (2000).

[12] P. Pohl, F. H. Renner, M. Eckardt, A. Schwanhausser, A. Friedrich, O. Yuksekdag, S. Malzer, G. H. Dohler, P. Kiesel, D. Driscoll, M. Hanson, and A. C. Gossard, Appl. Phys. Lett. **83**, 4035-4037 (2003).

[13] Hector Cotal, Chris Fetzer, Joseph Boisvert, Geoffrey Kinsey, Richard King, Peter Hebert, Hojun Yoon, and Nasser Karam, Energy Environ. Sci. **2**, 174 (2009).

[14] A. Guivarc'h, A. Le Corre, P. Auvray, B. Guenais, J. Caulet, Y. Ballini, R. Guerin, S. Deputier, M. C. Le Clanche, G. Jezequel, B. Lepine, A. Quemerais, and D. Sebilleau, J. Mater. Res. **10**, 1942–1952 (1995).

[15] M. W. Denhoff, J. Phys. D: Appl. Phys. **39**, 1761 (2006).

[16] C. Kadow, J. A. Johnson, K. Kolstad, and A. C. Gossard, J. Vac. Sci. Technol. B **21**, 29 (2003).

[17] Hari P. Nair, Adam M. Crook, and Seth R. Bank, submitted to Appl. Phys. Lett. (2009).